Virtual Knot Diagrams and the Witten-Reshetihken-Turaev Invariant

H. A. Dye
MADN-MATH
United States Military Academy
646 Swift Road
West Point, NY 10996
hdye@ttocs.org
Louis H. Kauffman
Department of Mathematics, Statistics, and Computer Science
University of Illinois at Chicago
851 South Morgan St
Chicago, IL 60607-7045
kauffman@uic.edu

Abstract

The Witten-Reshetihkin-Turaev invariant of classical knot diagrams is generalized to virtual knot diagrams. This invariant is unchanged by the framed Reidemeister moves and the Kirby calculus. The normalized Witten-Reshetihkin-Turaev invariant is unchanged by the Reidemeister moves and the Kirby calculus. As a result, it is also an invariant of the 3-manifolds represented by the classical knot diagrams. We generalize this invariant to virtual knot diagrams. This result is used to demonstrate that there are virtual knot diagrams with a non-trivial Witten-Reshetihkin-Turaev invariant and trivial fundamental group.

1

1   Introduction

Generalizations of the Jones polynomial have been defined for virtual link diagrams [**?**], [3], [11]. We continue this process by generalizing the Witten-Reshetihkin-Turaev invariant and the colored Jones polynomials to virtual link diagrams. The Witten-Reshetihkin-Turaev invariant of classical link diagrams is unchanged by the framed Reidemeister moves. It is also 3-manifold invariant and is unchanged by the Kirby calculus. This invariant is a weighted sum of colored Jones polynomials. Our generalization will also be a weighted sum of colored Jones polynomials and invariant under the framed Reidemeister moves and a generalization of the Kirby calculus.

Every framed, classical link diagram represents a 3-manifold via framed surgery performed on that link. Two 3-manifolds represented by link diagrams are homeomorphic if and only if their diagrams are related by a sequence of framed Reidemeister moves and Kirby calculus moves. The fundamental group of this 3-manifold can be computed from a corresponding link diagram. As a result, we can formally extend the definition of the 3-manifold group to a virtual link diagram. We define a virtual Kirby calculus by generalizing the moves of Kirby calculus to incorporate virtual crossings.

Surprisingly, the 3-manifold group of a virtual link diagram is invariant under the framed Reidemeister moves, the virtual Reidemeister moves, and the virtual Kirby calculus. This invariance gives rise to the concept of 'virtual 3-manifolds'. Virtual link diagrams appear to have the same structure as classical link diagrams (that specify 3-manifolds), but virtual 3-manifolds (specified by non-classical virtual diagrams) have no corresponding surgery construction. A virtual 3-manifold is, by definition, an equivalence class of link diagrams related by the framed Reidemeister moves, virtual Reidemeister moves, and virtual Kirby calculus.

In this paper, we recall virtual knot theory in section 2. We recall the definitions of the virtual fundamental group and the generalized Jones polynomial. Then, we define the 3-manifold group of a virtual link diagram using the definition of the virtual fundamental group. We prove that the 3-manifold group of a virtual link diagram is invariant under the framed Reidemeister moves, virtual Reidemeister moves and the Kirby calculus.

In section 3, we recall the definition of the colored Jones polynomial of a virtual link diagram. We use this definition to define the Witten-Reshetihkin-Turaev invariant of a virtual link diagram. We introduce several formulas that reduce the computational complexity of the Witten-Reshetihkin-Turaev invariant. Finally, we prove that the Witten-Reshetihkin-Turaev invariant is invariant under the Kirby calculus.

The reader should note that all formulas in the paper that are written in the form of a graphical equation are formulas that indicate the possibility of a substitution of one type of graphic for another graphic in a link diagram. The equality in the equation means that the bracket evaluation of the two diagrams are equal.

We compute the Witten-Reshetihkin-Turaev invariant of two virtual knot

diagrams in the next section. The fundamental group of these virtual knot diagrams is $\mathbb{Z}$. The 3-manifold group of one of the virtual knot diagrams is the trivial group. However, the Witten-Reshetihkin-Turaev invariant of this virtual knot diagrams is non-trivial. This produces a virtual counterexample to the Poincare conjecture.

In the final section, we discuss the difficulties of computing the Witten-Reshetihkin-Turaev invariant in the virtual case. We observe that in order to compute the Witten-Reshetihkin-Turaev invariant of a virtual link diagram, we must compute the Jones polynomial of some complicated virtual link diagrams. The formulas given in sections 3 and 4 were computed using Temperly-Lieb recoupling theory. The full machinery of recoupling theory does not generalize to the virtual case. We present several propositions that highlight the difficultly of computing formulas that include virtual crossings.

2   Virtual Knot Diagrams

Virtual knot theory is a generalization of classical knot theory introduced by Louis H. Kauffman in 1996 [8]. In this section, we review classical and virtual knot theory. We then recall several classical knot invariants that have been generalized to virtual knot diagrams.

A *classical knot diagram* is a decorated immersion of S^1 into the plane with over/under markings at each crossing. Two classical knot diagrams are said to be *equivalent* is one may be transformed into another by a sequence of Reidemeister moves. Local versions of the Reidemeister move are illustrated in figure 1.
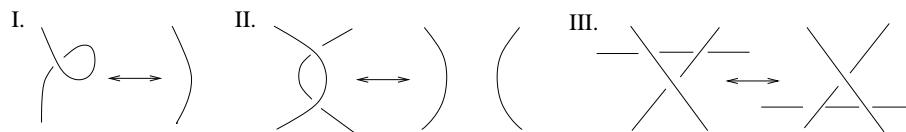

Figure 1: Reidemeister moves

A *virtual knot diagram* is a decorated immersion of S^1 into the plane with two types of crossings: classical and virtual. Classical crossings are indicated by over/under markings and virtual crossings are indicated by a solid encircled X. Two virtual knot diagrams are said to be *equivalent* if one may be transformed into the other via a sequence of Reidemeister moves and virtual Reidemeister moves. The *virtual Reidemeister moves* are illustrated in figure 2. Note that the classical knot diagrams are a subset of the virtual knot diagrams.
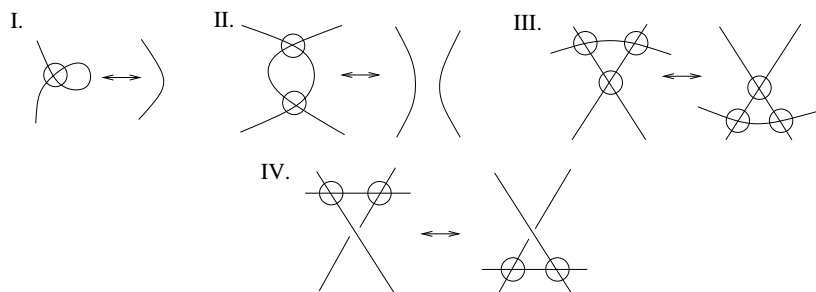

Figure 2: Virtual Reidemeister moves

The virtual Reidemeister moves can be constructed from a single diagrammatic move: the *detour move*. The detour move pertains only to virtual crossings and is performed in the following way. Choose an orientation of the virtual knot diagram for convenience. Select two points, a and b, on the virtual knot diagram. The arc from a to b, in the direction of the orientation, contains only virtual crossings and no classical crossings. Otherwise we may not perform the detour move. (This condition is illustrated in figure 3.) Remove the arc of the

knot diagram from point a to point b, and insert any new arc that does not create triple points. All double points produced by the placement of the new arc are virtual crossings.
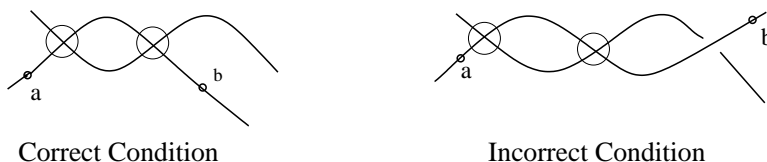

Correct Condition   Incorrect Condition

Figure 3: The detour move condition

Proposition 2.1. *The detour move is equivalent to a sequence of virtual Reidemeister moves.*

Remark 2.1. *We sketch the proof of this proposition. A large scale move like the detour move may be broken down in a series of smaller sequential moves. These smaller moves involve at most three crossings. Note that each virtual Reidemeister move is a detour move.*

Remark 2.2. *Equivalence classes of virtual knot diagrams are in one to one correspondence with equivalence classes of embeddings of S^1 into thickened, oriented 2-dimensional surfaces [6], [10] and [2]. A surface with an embedded S^1 is equivalent to a (possibly different) surface with an embedded S^1 if one surface with an embedding can be transformed into the other by a sequence of homeomorphisms of the surface, handle cancellations and additions (to the surface), and Reidemeister moves in the surface.*

A *virtual n-tangle diagram* is a decorated immersion of n copies of $[0, 1]$ with classical and virtual crossings. The $2n$ endpoints of the diagram are arranged so that n endpoints appear in a row at the top and n endpoints form a lower row. Note that it is possible to construct tangle diagrams with no crossings. The *closure* of an *n*-tangle, T connects each upper endpoint with a corresponding lower endpoint as illustrated in figure 4.
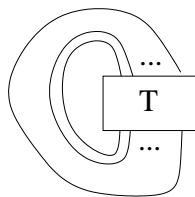

Figure 4: The closure of an n-tangle

We now recall the definition of several invariants of virtual knot diagrams. These invariants will be referred to throughout this paper. The *writhe* of a

virtual knot diagram and the *linking number* of a virtual link diagram are computed from an oriented diagram. To define these invariants, we introduce the *sign (crossing sign)* of a classical crossing. Each classical crossing in a virtual

$$+1 \qquad\qquad -1$$

Figure 5: Crossing sign

knot diagram can be assigned a *crossing sign*. To compute the crossing sign, we orient the knot diagram. Each classical crossing is assigned a $\pm$ value based on the orientation as shown in figure 5. Let v be a classical crossing in a virtual knot diagram. We denote the crossing sign of v as $sgn(v)$. The *writhe* of a virtual knot diagram K is determined by the crossing sign of each classical crossing in the diagram. We denote the writhe of K as $w(K)$.

$$w(K) = \sum_{v \in K} sgn(v)$$

The Reidemeister I move changes the writhe of a knot diagram. An unknot with a single Reidemeister I move, is referred to as ± 1 framed unknots based on the sign of the crossing. (We illustrate ± 1 framed unknots in figure 6.) The Reidemeister II and III moves do not change the writhe of a knot diagram and are referred to as the *framed Reidemeister moves*. Two classical knot diagrams that are related by a sequence of Reidemeister II and III moves are said to be *regularly isotopic*.
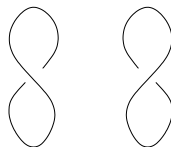

Figure 6: ± 1 Framed unknots

The *linking number* of an oriented two component virtual link diagram with oriented components, L_1 and L_2, is denoted $lk(L_1, L_2)$. Let U denote the set of all classical crossings formed by the components L_1 and L_2. Then the linking number is defined by the formula:

$$lk(L_1, L_2) = \sum_{v \in U} \frac{sgn(v)}{2}. \tag{1}$$

Note that $lk(L_1, L_2) = lk(L_2, L_1)$.

Remark 2.3. *There is an alternative definition of writhe where $lk(L_1, L_2)$ and $lk(L_2, L_1)$ are not necessarily equivalent [4].*

We recall the fundamental group and the longitude of a virtual knot diagram. These definitions are used to generalize the 3-manifold group obtained from a classical knot diagram to virtual knot diagrams.

The *fundamental group* of a virtual knot diagram is a free group modulo relations determined by the classical crossings in the diagram. Each *segment* of the diagram starts and terminates at classical crossings (possibly passing through virtual crossings). We assign each segment a label. These labels represent the generators of the free group. From each crossing we obtain a relation as illustrated in figure 7.
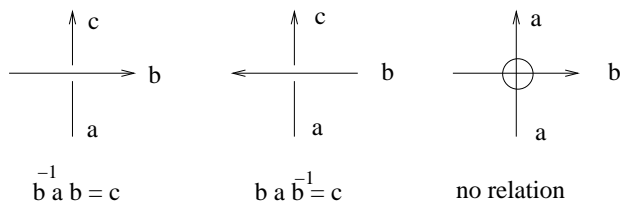

Figure 7: Relations determined by crossings

The fundamental group of a virtual knot diagram is invariant under the Reidemeister moves and virtual Reidemeister moves.

A *longitude* of a virtual knot diagram is word of the form $l_1^{\pm 1} l_2^{\pm 1} \ldots l_1^{\pm 1}$ where each l_i is one of the generators of the fundamental group. We compute a longitude by choosing an initial point on the diagram. We traverse the virtual knot diagram from the initial point in the direction of its orientation. We record either b or b^{-1} as we traverse an underpass under the arc b. We determine whether to record b or b^{-1} as shown in figure 8. The longitude of a virtual knot diagram is determined up to cyclic permutation of its members.
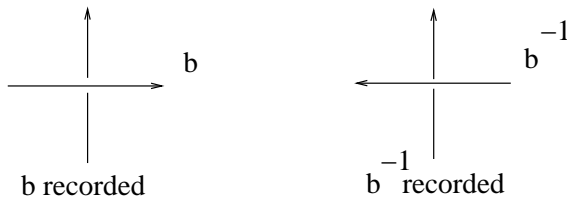

Figure 8: Longitude determined by crossings

The *three-manifold group* of a virtual knot diagram K, $\pi_M(K)$, is the fundamental group modulo the longitude. The three-manifold group is invariant under the Reidemeister moves II and III, the virtual Reidemeister moves, and the Kirby calculus. The *virtual Kirby calculus* consists of two moves: the introduction and deletion of ± 1 framed unknots and handle sliding. We describe a

handle slide for a framed virtual link diagram K with at least two components, A and B. Diagrammatically, handle slide A over B by the following process. Replace B with two parallel copies of B. Take the connected sum of A and the outermost copy of B.

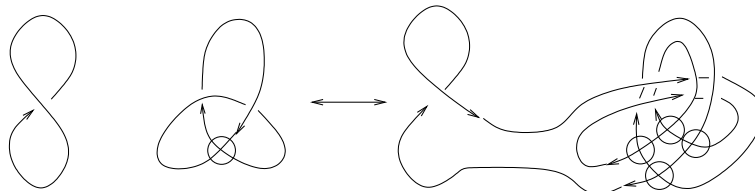We show an example of this process in figure 9, where a +1 framed unknot is slid over a trefoil.

Figure 9: A example of a handle slide with virtual crossings

These two moves are called the *Kirby moves*.

Remark 2.4. *In the case of classical link diagrams, the definition of the classical Kirby calculus is identical to the definition given above without virtual crossings.*

Remark 2.5. *The following question has been posed: if two classical diagrams are equivalent under the virtual Kirby calculus, are they equivalent under the classical Kirby calculus.*

The 3-manifold group is invariant under the framed Reidemeister moves and the virtual Reidemeister moves. It remains to prove that the 3-manifold group is invariant under the Kirby moves.

A classical framed link diagram represents the three manifold obtained by removing a small neighborhood of each component of the link diagram, and gluing in a solid torus so that the meridian is identified with the longitude of the removed link component [12]. The Reidemeister I move changes the longitude of a knot diagram and changes the identification used to glue in the torus.

For example, the fundamental group of an unknot with writhe 0 and the fundamental group of a ± 1 framed unknot are both $\mathbb{Z}$. However, the 3-manifold group of an unknot with writhe zero is $\mathbb{Z}$ and the three-manifold group of the ± 1 framed unknot is the trivial group. The unknot with writhe 0 represents $S^1 \times S^2$ and the ± 1 framed unknot represents S^3.

Theorem 2.2. *If two classical framed link diagrams, K and $\hat{K}$, are related by a sequence of Kirby moves and framed Reidemeister moves then*

$$\pi_M(K) = \pi_M(\hat{K})$$

and the two diagrams represent homeomorphic three manifolds.

Proof: [12]. ∎

Theorem 2.3. *The 3-manifold group of a virtual knot diagram K, is invariant under the framed Reidemeister moves, the virtual Reidemeister moves (detour move) and the Kirby calculus.*

Proof: The fundamental group is not changed by the framed Reidemeister moves and the virtual Reidemeister moves. The longitude is also unchanged by the Reidemeister II and III moves and the detour move. This implies that the 3-manifold group of a virtual knot diagram is not changed by these moves. We only need to show that the 3-manifold group is unchanged by the Kirby moves.

The 3-manifold group of a ± 1 framed unknot is trivial and the introduction of a disjoint ± 1 framed unknot to the diagram does not change the 3-manifold group.

We consider the effect of handle sliding on a virtual knot diagram. Consider a virtual knot diagram with two disjoint components, oriented as shown in figure 10. Denote the two components by K_1 and K_2, the 3-manifold group by $\pi_M(K_1 \amalg K_2)$, and the longitudes of K_1 and K_2 as L_1 and L_2. Assume that the arcs of K_1 are labeled sequentially as $Z, Z_1, Z_2 \ldots Z_m$ in the direction of orientation. The placement of the labeled arc Z is indicated in figure 10. Similarly, the arcs of the component K_2 are labeled in the direction of orientation as $A_1, A_2, \ldots A_n$. (To generalize the argument, we would consider the different possible orientations of K_1 and K_2, and the case where K_2 is a link with multiple components.)
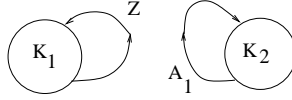

Figure 10: Two virtual knot diagrams before a handle slide

Handle slide K_1 over K_2, and we obtain the diagram shown in figure 11. Let $\hat{K}$ denote the new diagram, $\pi_M(\hat{K})$ the corresponding 3-manifold group, and $\hat{L}_1$ and $\hat{L}_2$ the new longitudes.
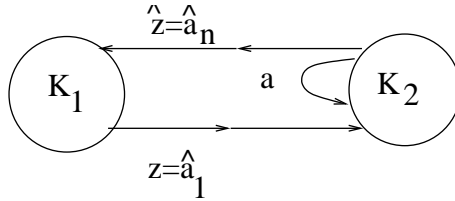

Figure 11: Two virtual knot diagrams after a handle slide

The virtual crossings do not produce any new relations, therefore we need only examine the effect of the handle slide on the classical crossings. Each original crossing in K_1 is unchanged. Each classical crossing in K_2 becomes a set of four classical crossings whose four relations reduce to a single equation. Consider a positive crossing in K_2 as shown in figure 12.
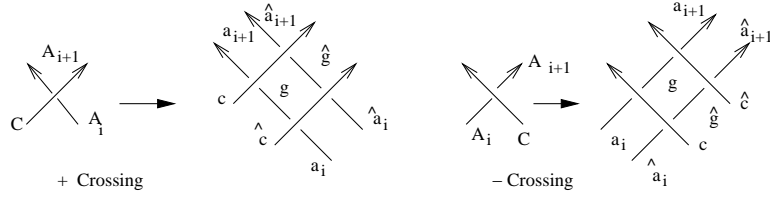
Figure 12: Detail of of a crossing before and after a handle slide

We obtain the following relationship from a positive classical crossing before handle sliding: $C^{-1}A_iC = A_{i+1}$. After handle sliding, we obtain four relations from the positive crossing.

$$c^{-1}gc = a_{i+1} \qquad c^{-1}\hat{g}c = \hat{a}_{i+1}$$
$$\hat{c}^{-1}a_i\hat{c} = g \qquad \hat{c}^{-1}\hat{a}_i\hat{c} = \hat{g}$$

These equations may be simplified to two equations:

$$c^{-1}\hat{c}^{-1}a_i\hat{c}c = a_{i+1}$$
$$c^{-1}\hat{c}^{-1}\hat{a}_i\hat{c}c = \hat{a}_{i+1}$$

Multiplying, we obtain a single relation from each set of four positive crossings:

$$(\hat{c}c)^{-1}(\hat{a}_ia_i)(\hat{c}c) = \hat{a}_{i+1}a_{i+1}$$

The change for negative classical crossing is also shown in figure 12. We also obtain a single relation in the case of a negative crossing.

$$(\hat{c}c)(\hat{a}_ia_i)(\hat{c}c)^{-1} = \hat{a}_{i+1}a_{i+1}$$

Consider the longitude of K_2. Compute the original longitude by traversing the knot starting at A_1. If $L_2 = \{x_1^{\pm 1}, x_2^{\pm 1} \ldots x_n^{\pm 1}\}$ then

$$\hat{L}_2 = \{(\hat{x_1}x_1)^{\pm 1}, (\hat{x_2}x_2)^{\pm 1} \ldots (\hat{x_n}x_n)^{\pm 1}\}.$$

Hence, $\hat{L}_2 a_1 z \hat{L}_2^{-1} = a_1 \hat{z}$ implies that $z = \hat{z}$. Further, if L_1 is computed by traversing the knot from z in the direction of the orientation, then we observe that $\hat{L}_1 = L_1\hat{L}_2$. These computations allow us to conclude that $\pi_M(K) = \pi_M(\hat{K})$. ∎

We recall a generalization of the bracket model [7] to define the *generalized Jones polynomial* of a virtual knot diagram. Each classical crossing may be *smoothed* as a type α smoothing or a type β smoothing as illustrated in figure 13.

A *state* of a virtual knot diagram is a diagram determined by a choice of smoothing type for each classical crossing. Note that a state of a virtual link diagram may contain virtual crossings and consists of closed curves (possibly) with virtual crossings.
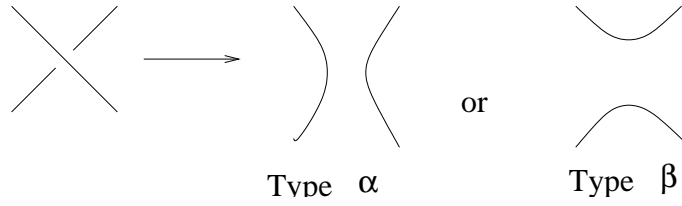
Figure 13: Smoothing types

Let K be a virtual knot diagram. Let s be a state of the virtual knot diagram, let S represent the set of all possible states and let $c(s)$ equals the number of type β crossings minus the number of type α crossings. Let $|s|$ denote the number of closed curves in the smoothed diagram and $d = -(A^2 + A^2)$. The bracket polynomial of K denoted $\langle K \rangle$ then:

$$\langle K \rangle = \sum_{s \in S} d^{|s|-1} A^{c(s)}$$

The bracket polynomial is invariant under the Reidemeister II and III moves and the virtual Reidemeister moves. To obtain invariance under the Reidemeister I move, we use the writhe of K to normalize. We define the *normalized bracket polynomial* of a virtual knot diagram.

$$f_K(A) = (-A)^{-3w(k)} \langle K \rangle$$

The only difference between this definition and the definition of the classical Jones polynomial is that a state of virtual knot diagram is set of closed curves (possibly containing virtual crossings) and not a set of simple closed curves. The *Jones polynomial*, $V_K(t)$, and the bracket polynomial are related by letting $A = t^{-1/4}$.

$$f_K(t^{1/4}) = V_K(t) \tag{2}$$

In the next section, we introduce the Witten-Reshetihkin-Turaev invariant. This invariant will be generalized to virtual knot diagrams and is invariant under the Kirby calculus, framed Reidemeister moves, and the virtual Reidemeister moves.

3   The Witten-Reshetikhin-Turaev Invariant

In this section, we extend the definition of the Witten-Reshetikhin-Turaev invariant [15], [13], [14] to virtual link diagrams. First, we recall the definition of the Jones-Wenzl projector (q-symmetrizer)[9]. We then define the colored Jones polynomial of a virtual link diagram. It will be clear from this definition that two equivalent virtual knot diagrams have the same colored Jones polynomial. We will use these definitions to extend the Witten-Reshetikhin-Turaev invariant to virtual link diagrams. From this construction, we conclude that two virtual link diagrams, related by a sequence of framed Reidemeister moves and virtual Reidemeister moves, have the same Witten-Reshetikhin-Turaev invariant. Finally, we will prove that the generalized Witten-Reshetikhin-Turaev invariant is unchanged by the virtual Kirby calculus. In the next section, we present two virtual knot diagrams that have fundamental group $\mathbb{Z}$ and a Witten-Reshetikhin-Turaev invariant that is not equivalent to 1.

To form the *n-cabling* of a virtual knot diagram, take n parallel copies of the virtual knot diagram. A single classical crossing becomes a pattern of n^2 classical crossings and a single virtual crossing becomes n^2 virtual crossings.

Let r be a fixed integer such that $r \geq 2$ and let

$$A = e^{\frac{\pi i}{2r}}.$$

Here is a formula used in the construction of the Jones-Wenzl projector.

$$\Delta_n = (-1)^n \frac{A^{2n+2} - A^{-(2n+2)}}{A^2 - A^{-2}}.$$

Note that $\Delta_1 = -(A^2 + A^{-2})$, the value assigned to a simple closed curve by the bracket polynomial. There will be an an analogous interpretation of Δ_n which we will discuss later in this section.

We recall the definition of an n-tangle. Any two n-tangles can be multiplied by attaching the bottom n strands of one n-tangle to the upper n strands of another n-tangle. We define an n-tangle to be *elementary* if it contains to no classical or virtual crossings. Note that the product of any two elementary tangles is elementary. Let I denote the identity n-tangle and let U_i such that $i \in \{1, 2, \ldots n-1\}$ denote the n-tangles shown in figure 14. By multiplying
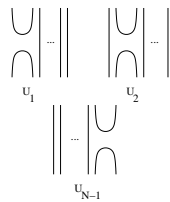

Figure 14: Elementary n-tangles

a finite set of $U_{i_1} U_{i_2} \ldots U_{i_n}$, we can obtain any elementary n-tangle. Formal

sums of the elementary tangles over $\mathbb{Z}[A, A^{-1}]$ generate the nth Temperly-Lieb algebra [9].

We recall that the nth *Jones-Wenzl projector* is a certain sum of all elementary n-tangles with coefficients in $\mathbb{C}$. We denote the nth Jones Wenzl projector as T_n. We indicate the presence of the Jones-Wenzl projector and the n-cabling by labeling the component of the knot diagram with n.

Remark 3.1. *There are different methods of indicating the presence of a Jones-Wenzl projector. In a virtual knot diagram, the presence of the nth Jones-Wenzl projector is indicated by a box with n strands entering and n strands leaving the box. For n-cabled components of a virtual link diagram with a attached Jones-Wenzl projector, we indicate the cabling by labeling the component with n and the presence of the projector with a box. This notation can be simplified to the convention indicated in the definition of the the colored Jones polynomial. The choice of notation is dependent on the context.*

We construct the Jones-Wenzl projector recursively. The 1st Jones-Wenzl projector consists of a single strand with coefficient 1. The is exactly one 1-tangle with no classical or virtual crossings. The nth Jones-Wenzl projector is constructed from the $(n-1)^{th}$ and $(n-2)^{th}$ Jones-Wenzl projectors as illustrated in figure 15.
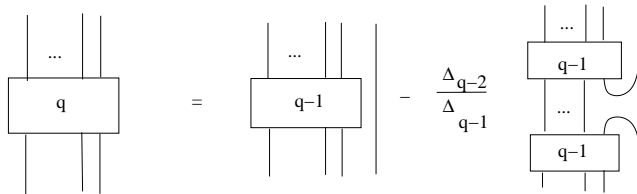

Figure 15: n^{th} Jones-Wenzl Projector

We use this recursion to construct the 2nd Jones-Wenzl projector as shown in figure 16.
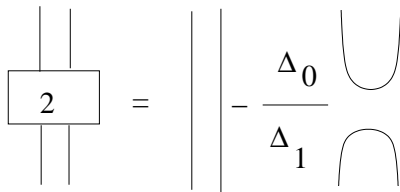

Figure 16: 2nd Jones-Wenzl Projector

We will refer to the Jones-Wenzl projector as the J-W projector for the remainder of this paper.

We review the properties of the J-W projector. Recall that T_n denotes the

n^{th} J-W projector then

$$\text{i) } T_n T_m = T_n \text{ for } n \geq m$$
$$\text{ii) } T_n U_i = 0 \text{ for all } i$$
$$\text{iii) The bracket evaluation of the closure of } T_n = \Delta_n$$

Remark 3.2. *The combinatorial definition of the J-W projector is given in [9], p. 15. Note that [9] provides a full discussion of all formulas given above.*

Let K be a virtual link diagram with components $K_1, K_2 \ldots K_n$. Fix an integer $r \geq 2$ and let $a_1, a_2 \ldots a_n \in \{0, 1, 2, \ldots r-1\}$. Let $\bar{a}$ represent the vector $(a_1, a_2, \ldots a_n)$. Fix $A = e^{\frac{\pi i}{2r}}$ and $d = -A^2 - A^{-2}$. We denote the *generalized $\bar{a}$ colored Jones polynomial* of K as $\langle K^{\bar{a}} \rangle$. To compute $\langle K^{\bar{a}} \rangle$, we cable the component K_i with a_i strands and attach the a_i^{th} J-W projector to cabled component K_i. We apply the Jones polynomial to the cabled diagram with attached J-W projectors.

The colored Jones polynomial is invariant under the framed Reidemeister moves and the virtual Reidemeister moves. This result is immediate, since the Jones polynomial is invariant under the framed Reidemeister moves and the virtual Reidemeister moves.

Remark 3.3. *The a-colored Jones polynomial of the unknot is Δ_a. In other words, the Jones polynomial of the closure of the ath J-W projector is Δ_a.*

The *generalized Witten-Reshetikhin-Turaev invariant* of a virtual link diagram is a sum of colored Jones polynomials. Let K be a virtual knot diagram with n components. Fix an integer $r \geq 2$. We denote the unnormalized Witten-Reshetikhin Turaev invariant of K as $\langle K^{\omega} \rangle$, which is shorthand for the following equation.

$$\langle K^{\omega} \rangle = \sum_{\bar{a} \in \{0,1,2,\ldots r-1\}^n} \Delta_{a_1} \Delta_{a_2} \ldots \Delta_{a_n} \langle K^{\bar{a}} \rangle \tag{3}$$

Remark 3.4. *For the remainder of this paper, the Witten-Reshetikhin-Turaev invariant will be referred to as the WRT.*

We define the matrix N in order to construct the normalized WRT. The normalization is chosen so that the the WRT of a ± 1 framed unknot is 1. Let N be the matrix defined as follows:

$$\text{i) } N_{ij} = lk(K_i, K_j) \text{ for } i \neq j$$
$$\text{ii) } N_{ii} = w(K_i)$$

then let

$$b_+(K) = \text{ the number of positive eigenvalues of } N$$
$$b_-(K) = \text{ the number of negative eigenvalues of } N$$
$$n(k) = b_+(K) - b_-(K).$$

The normalized WRT of a virtual link diagram K is denoted as $Z_K(r)$. Let $A = e^{\frac{\pi i}{2r}}$ and let $|k|$ denote the number of components in the virtual link diagram K. Then $Z_K(r)$ is defined by the formula

$$Z_K(r) = \langle K^\omega \rangle \mu^{|K|+1} \alpha^{-n(K)}$$

where

$$\mu = \sqrt{\frac{2}{r}} sin(\frac{\pi}{r})$$

and

$$\alpha = (-i)^{r-2} e^{i\pi[\frac{3(r-2)}{4r}]}.$$

We demonstrate that the normalized, generalized WRT is invariant under the framed Reidemeister moves and the Kirby calculus. The WRT is a sum of colored Jones polynomials and it is clear that the WRT is invariant under the framed Reidemeister moves and the virtual Reidemeister moves. The normalized WRT is invariant under first Kirby move (the introduction and deletion of ± 1 framed unknots) because the normalized WRT of this knot diagram is 1.

Theorem 3.1. *Let K be a virtual link diagram then $\langle K^\omega \rangle$ is invariant under the framed Reidemeister moves, virtual Reidemeister moves, and the virtual Kirby calculus.*

In the next few subsections, we introduce some necessary machinery.

In the classical case, the computation of this invariant is simplified by the use of recoupling theory. In the next section, we introduce formulas from recoupling theory [9]. Recoupling theory establishes a relationship between labeled knot diagrams and labeled trivalent graphs with classical and virtual crossings. These formulas allow us to compute the WRT without a full expansion of the Jones polynomial.

3.1 Kirby Calculus Invariance

These formulas are obtained from recoupling theory at roots of unity [9]. The formulas simplify the computation of the WRT. They will be used to prove that the WRT is invariant under Kirby calculus.

Consider a virtual link diagram with components: $K_1, K_2 \ldots K_n$. We cable component K_i with a_i strand and attach a J-W projector. This virtual link diagram can be regarded as a collection of labeled trivalent graphs (each with one edge and no vertices) with classical and virtual crossings. We introduce some formulas obtained from recoupling theory. These formulas describe identities between sums of bracket evaluations of labeled trivalent graphs. A full derivation of each formula can be obtained in [9].

Given a trivalent vertex with labels a, b, and c coming into the vertex, we translate this into an expression of J-W projectors. We connect the internal lines as indicated in figure 17. Note that $i + j = a$, $j + k = b$, and $k + i = c$

where i, j, and k are non-negative integers. In order for such a construction to be made: $a + b + c$ is even, $a + b - c \geq 0$, $b + c - a \geq 0$, and $c + a - b \geq 0$. These conditions are an admissibilty condition for translating any trivalent vertex into projectors for evaluating the colored Jones polynomial for any value of $\bar{a}$. We now give a more technical definition of admissibility for evaluation at roots of unity.
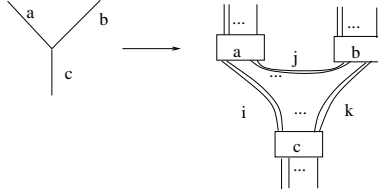

Figure 17: Associating projectors to a trivalent vertex

Fix an integer $r \geq 2$ and let $A = e^{\frac{\pi i}{2r}}$. The *quantum factorial* is a factorial product based on Δ_n. Let $0 \leq m \leq r - 1$. The mth quantum factorial is denoted by $[m]!$. Now,

$$[n] = (-1)^{n-1} \Delta_{n-1}$$
$$[0]! = 1 \text{ and } [1]! = \Delta_0$$
$$[m]! = [m][m-1]\ldots[1].$$

For r, an *admissible triple* is a set of three non-negative integers such that:

$$\text{i)} a + b + c \text{ is even}$$
$$\text{ii) } a + b - c \leq 2r - 4$$
$$\text{iii) } a + c - b \leq 2r - 4$$
$$\text{iv) } b + c - a \leq 2r - 4$$

We recall the θ-net formula, $\theta(a, b, c)$. Let a, b, c be an admissible triple and let $m = \frac{a+b-c}{2}$, $n = \frac{a+c-b}{2}$, and $p = \frac{b+c-a}{2}$ then

$$\theta(a, b, c) = (-1)^{m+n+p} \frac{[m+n+p+1]![m]![n]![p]!}{[m+n]![n+p]![p+m]!} \tag{4}$$

The labeled trivalent diagram shown in figure 18 is referred to as a θ-net. The virtual link diagram represented by the θ-net diagram is pictured on the right (by using the prescription for replacing trivalent vertices with projectors and reducing them). The Jones polynomial of this virtual link diagram is $\theta(a, b, c)$.

Note that we can only construct the link diagram corresponding to a θ-net if (a, b, c) is an admissible triple.

The formula shown in figure 19 (a special case of the recoupling formulas from section 5) expresses the fact that the bracket evaluation of a diagram
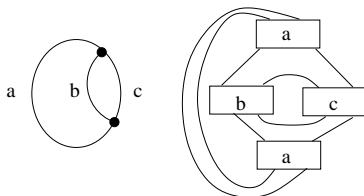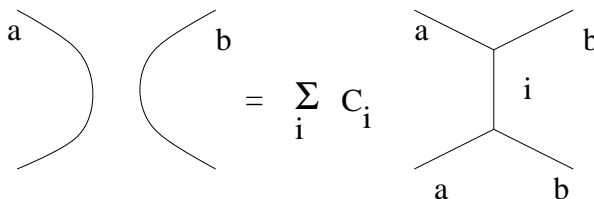
Figure 18: θ-Net Graph

Figure 19: Graph fusion

with two nearby arcs can be replaced with the bracket evaluation of the sum of diagrams obtained by the indicated graphical insertion.

The coefficients C_i in this sum are:

$$C_i = \frac{\Delta_i}{\theta(a,b,i)}. \tag{5}$$

We can only construct the corresponding virtual link diagram when (a,b,i) is an admissible triple.

These formulas simplify the computation of the WRT of a virtual link diagram.

To prove that the WRT of a virtual knot diagrams is unchanged by the virtual Kirby calculus, we need only demonstrate the WRT is unchanged by handle sliding. We prove the following lemma:

Lemma 3.2. *Suppose that $\langle K^\omega \rangle$ satisfies the conditions shown in figure 20. Then $\langle K^\omega \rangle$ is invariant under handle sliding.*

Proof:

Let K_1 and K_2 be two disjoint components of a virtual knot diagram. Let G_1 denote the cabled $K \amalg \hat{K}$ with J-W projectors attached as illustrated in figure 21.

We handle slide K_1 over the knot K_2 to obtain the diagram G_4. We will show that $\langle G_1^\omega \rangle = \langle G_4^\omega \rangle$.

Fix $r \geq 2$ and let $I = \{0, 1, \ldots r - 1\}$. Then:

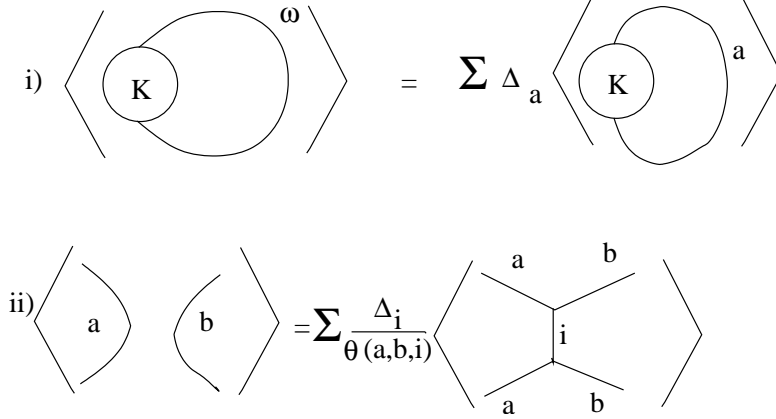$$\langle G_1^\omega \rangle = \sum_{a,b \in I} \Delta_a \Delta_b \langle (K_1 \amalg K_2)^{(a,b)} \rangle.$$

17

Figure 20: Conditions for Lemma 3.2

Fix a and consider the sum:

$$\sum_{b \in I} \Delta_a \Delta_b \langle (K_1 \amalg K_2)^{(a,b)} \rangle \tag{6}$$
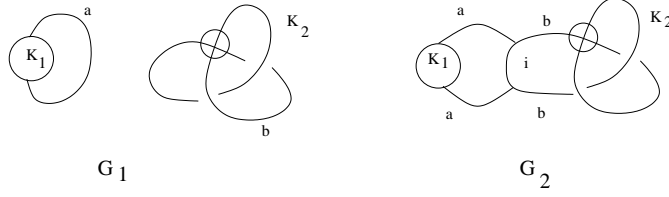

Figure 21: Recoupling move for the handle slide

Perform fusion on K_1 and K_2 and obtain the new diagram G_2. Now:

$$\sum_{b \in I} \Delta_a \Delta_b \langle G_1^{(a,b)} \rangle = \sum_{b \in I} \Delta_a \Delta_b \sum_{i \in I} \frac{\Delta_i}{\theta(a,b,i)} \langle G_2^{(a,b,i)} \rangle$$

We slide the upper vertex of this graph until we obtain the diagram G_3 as shown in figure 22. Sliding this edge corresponds to a sequence of Reidemeister II, III and virtual Reidemeister moves.

As a result,

$$\sum_{b \in I} \Delta_a \Delta_b \langle G_1^{(a,b)} \rangle = \sum_{b,i \in I} \frac{\Delta_a \Delta_b \Delta_i}{\theta(a,b,i)} \langle G_3^{(a,b,i)} \rangle \tag{7}$$

Applying the inverse of the fusion formula to the previous equation:

$$\sum_{b \in I} \Delta_a \Delta_b \langle G_1^{(a,b)} \rangle = \sum_{i \in I} \Delta_a \Delta_i \langle G_4^{(a,i)} \rangle$$
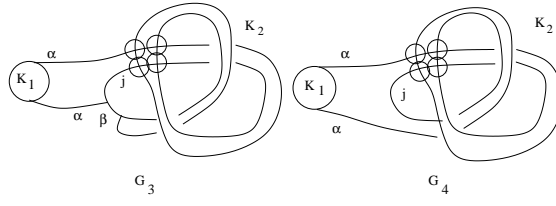
18

Figure 22: Recoupling diagrams after fusion

Now:

$$\sum_{a,b\in I}\Delta_a\Delta_b\langle G_1^{(a,b)}\rangle = \sum_{a,i\in I}\langle G_4^{(a,i)}\rangle \tag{8}$$

Hence, $\langle G_1^{(\omega,\omega)}\rangle = \langle G_4^{(\omega,\omega)}\rangle$. ∎

4 Examples

In this section, we compute the WRT of the two virtual knot diagrams, K and $\hat{K}$, shown in figure 23.
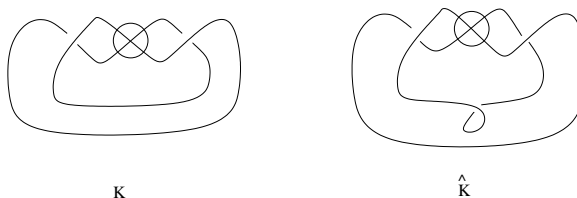

Figure 23: Virtual knot diagrams, K and $\hat{K}$

The three-manifold groups of these diagrams are

$$\pi_M(K) = \mathbb{Z} \text{ and } \pi_M(\hat{K}) = 1.$$

Note that $\pi_M(S^1 \times S^2) = \mathbb{Z}$ and $\pi_M(S^3) = 1$.

To compute the WRT of these virtual knot diagrams, we recall the following formulas from recoupling theory. These formulas establish a correspondence between labeled trivalent graphs and sums of virtual knot diagrams with coefficients in $\mathbb{C}$.

We define the *tetrahedral net* formula. Let a, b, c, d, e and f be non-negative integers.

$$Tet \begin{bmatrix} a & b & e \\ c & d & f \end{bmatrix} = \frac{G}{E} \prod_{m \leq s \leq M} \frac{(-1)^s[s+1]!}{\prod_i [s-a_i]!\pi_j[b_j - s]!} \tag{9}$$

such that

$$E = [a]![b]![c]![d]![e]![f]! \qquad G = \prod_{i,j}[b_j - a_i]!$$

$$a_1 = \frac{(a+d+e)}{2} \qquad\qquad a_2 = \frac{(b+c+e)}{2}$$

$$a_3 = \frac{(a+d+f)}{2} \qquad\qquad a_4 = \frac{(b+c+f)}{2}$$

$$b_1 = \frac{(a+c+e+f)}{2} \qquad b_2 = \frac{(b+d+e+f)}{2}$$

$$b_3 = \frac{(a+b+c+d)}{2}$$

$$m = min\{a_1, a_2, a_3, a_4\} \qquad M = max\{b_1, b_2, b_3\}$$

The trivalent graph shown on the left in figure 24 corresponds to the link diagram shown on the right. The Jones polynomial of this virtual link diagram is

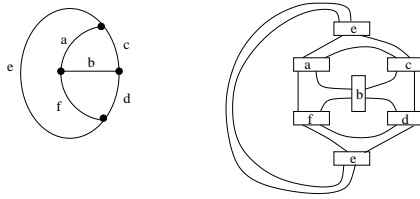$$Tet \begin{bmatrix} a & b & e \\ c & d & f \end{bmatrix}. \tag{10}$$

20

Figure 24: Tetrahedral net graph

We may remove a classical crossing from a trivalent graph using the following formula. We define the weight coefficient:

$$\lambda_c^{ab} = (-1)^{\frac{a+b-c}{2}} A^{\frac{a(a+2)+b(b+2)-c(c+2)}{2}}.$$

The complex conjugate of λ_c^{ab} is :

$$\bar{\lambda}_c^{ab} = (-1)^{\frac{a+b-c}{2}} A^{-\frac{a(a+2)+b(b+2)-c(c+2)}{2}}. \qquad (11)$$

We remove a simple twist from the diagram as shown in figure 25. The equalities indicate that the bracket evaluations of the two diagrams are equivalent.
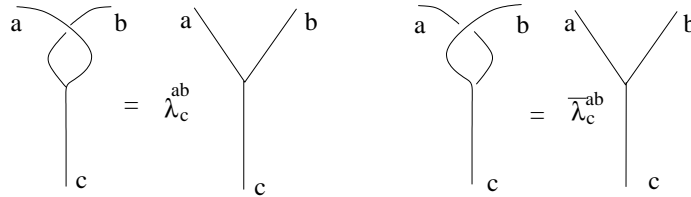

Figure 25: Graphical λ_c^{ab}

We may also simplify a trivalent graph using the formula shown in figure 26. We refer to this simplification as a bead removal.
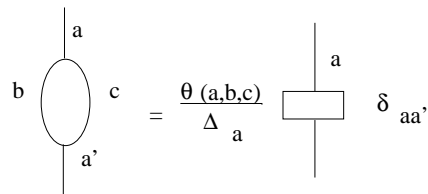

Figure 26: Bead removal formula

The following formula equates a classical crossing with a weighted sum of trivalent subgraphs. We exchange a crossing for a sum of trivalent subgraphs as shown in figure 27,
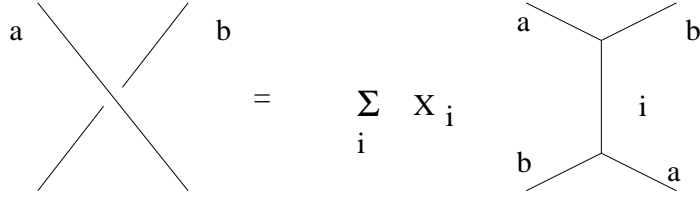
Figure 27: Crossing expansion formula

where

$$X_i = \frac{\Delta_i \lambda_i^{ab}}{\theta(a, b, i)}.$$

4.1   Computations

Let K and $\hat{K}$ be the diagrams shown in figure 23. We compute $\langle K^\omega \rangle$ and $\langle \hat{K}^\omega \rangle$. Applying the definition of the WRT,

$$\langle K^\omega \rangle = \sum_a \Delta_a \langle K^a \rangle$$

$$\langle \hat{K}^\omega \rangle = \sum_a \Delta_a \langle \hat{K}^a \rangle$$

Now, we use the formulas obtained from recoupling theory to transform the virtual knot diagrams K and $\hat{K}$ into the trivalent graph G shown in figure 28. As a result:

$$\langle K^\omega \rangle = \sum_{i,j,a} \Delta_a \frac{\Delta_i \Delta_j}{\theta(a,a,i)\theta(a,a,j)} \lambda_i^{aa} \lambda_j^{aa} \langle G \rangle$$

$$\langle \hat{K}^\omega \rangle = \sum_{i,j,a} \Delta_a \frac{\Delta_i \Delta_j}{\theta(a,a,i)\theta(a,a,j)} \lambda_i^{aa} \lambda_j^{aa} \lambda_0^{aa} \langle G \rangle.$$

Note that (a, i, j) is not an admissible triple unless $i = j$. Then:

$$\langle K^\omega \rangle = \sum_{i,a} \Delta_a \frac{\Delta_i^2 (\lambda_i^{aa})^2}{\theta(a,a,i)^2} \langle G \rangle$$

$$\langle \hat{K}^\omega \rangle = \sum_{i,a} \Delta_a \frac{\Delta_i^2}{\theta(a,a,i)^2} (\lambda_i^{aa})^2 \lambda_0^{aa} \langle G \rangle$$

Applying the θ-net identity, we obtain the graph, G', shown in figure 29.
    Now,

$$\langle K^\omega \rangle = \sum_{i,a} \Delta_a \frac{\Delta_i}{\theta(a,a,i)} (\lambda_i^{aa})^2 \langle G' \rangle$$

$$\langle \hat{K}^\omega \rangle = \sum_{i,a} \Delta_a \frac{\Delta_i}{\theta(a,a,i)} (\lambda_i^{aa})^2 \lambda_0^{aa} \langle G' \rangle$$
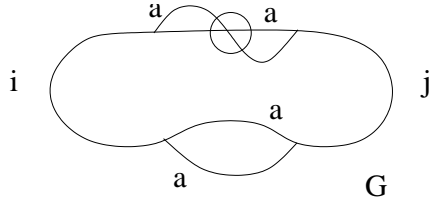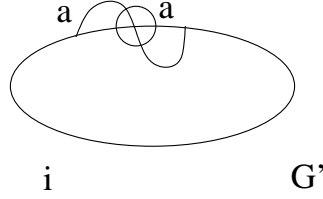
Figure 28: Graph obtained from K and $\hat{K}$

Figure 29: Reduced graph obtained from G

We determine for which values the triple, (a, a, i), is admissible. We then compute the Jones polynomial of the virtual link diagrams corresponding the the labeled graph, G'.

We indicate these values in table 2. If the triple (a, a, i) is not admissible, we have entered a zero in the corresponding table entry.

For $r = 3$:

$$\langle K^{\omega} \rangle = \frac{\Delta_0^2 (\lambda_0^{00})^2 \langle G' \rangle}{\theta(0,0,0)} + \frac{\Delta_0^2 (\lambda_0^{11})^2 \langle G' \rangle}{\theta(1,1,0)}$$

and

$$\langle \hat{K}^{\omega} \rangle = \frac{\Delta_0^2 (\lambda_0^{00})^3 \langle G' \rangle}{\theta(0,0,0)} + \frac{\Delta_0^2 (\lambda_0^{11})^3 \langle G' \rangle}{\theta(1,1,0)}.$$

Now,

$$\langle K^{\omega} \rangle = 0$$
$$\langle \hat{K}^{\omega} \rangle = 1 + i$$

We fix $r = 4$. We determine for what values (a, a, i) is an admissible triple. We then compute the Jones polynomial of the virtual link diagram corresponding to the graph G_2.

	$a = 0$	$a = 1$	$a = 2$
$i = 0$	1	$-A^2 - A^{-2}$	0
$i = 1$	0	0	0
$i = 2$	0	$-A^2 - A^{-2}$	0

Table 1: Jones polynomial of the graph G', $r = 3$

	$a = 0$	$a = 1$	$a = 2$	$a = 3$
$i = 0$	1	$-A^2 - A^{-2}$	$(-A^2 - A^{-2})^2$	0
$i = 1$	0	0	0	0
$i = 2$	0	$-A^2 - A^{-2}$	$(-A^2 - A^{-2})^2$	$(-A^2 - A^{-2})^2$
$i = 3$	0	0	0	0

Table 2: Jones polynomial of the graph G', $r = 4$

We compute $\langle K^\omega \rangle$ when $r = 4$.

$$\langle K^\omega \rangle = \frac{\Delta_0^2 (\lambda_0^{00})^2 \langle G' \rangle}{\theta(0,0,0)} + \frac{\Delta_0^2 (\lambda_0^{11})^2 \langle G' \rangle}{\theta(1,1,0)}$$
$$+ \frac{\Delta_0^2 (\lambda_0^{22})^2 \langle G' \rangle}{\theta(2,2,0)} + \frac{\Delta_2^2 (\lambda_2^{11})^2 \langle G' \rangle}{\theta(1,1,2)}$$
$$+ \frac{\Delta_2^2 (\lambda_2^{22})^2 \langle G' \rangle}{\theta(2,2,2)} + \frac{\Delta_2^2 (\lambda_2^{33})^2 \langle G' \rangle}{\theta(3,3,2)}$$

Similarly, we compute the WRT of $\hat{K}$ when $r = 4$.

$$\langle \hat{K}^\omega \rangle = \frac{\Delta_0^2 (\lambda_0^{00})^3 \langle G' \rangle}{\theta(0,0,0)} + \frac{\Delta_0^2 (\lambda_0^{11})^3 \langle G' \rangle}{\theta(1,1,0)}$$
$$+ \frac{\Delta_0^2 (\lambda_0^{22})^3 \langle G' \rangle}{\theta(2,2,0)} + \frac{\Delta_2^2 (\lambda_2^{11})^2 \lambda_0^{11} \langle G' \rangle}{\theta(1,1,2)}$$
$$+ \frac{\Delta_2^2 (\lambda_2^{22})^2 \lambda_0^{22} \langle G' \rangle}{\theta(2,2,2)} + \frac{\Delta_2^2 (\lambda_2^{33})^2 \lambda^{33} \langle G' \rangle}{\theta(3,3,2)}$$

We determine that

$$\langle K \rangle = 1.29289 + 1.70711i$$
$$\langle \hat{K} \rangle = 1.23044 + 0.92388i$$

The virtual knot diagram K has $b_+(K) = 0$ and $b_-(K) = 0$ implying $n(K) = -1$. Now, we normalize the WRT and determine that:

$$Z_K(3) = 0$$
$$Z_{\hat{K}}(3) = 0.707107i$$

We determine that the normalized WRT when $r = 4$.

$$Z_K(4) = -0.331106 + 0.92388i$$
$$Z_{\hat{K}}(4) = -0.331106 + 0.195807i$$

24

5   Recoupling Theory and Virtual Knot Diagrams

Recall the recoupling theorem [9].

Theorem 5.1 (Recoupling Theorem). *A single labeled trivalent graph is equivalent to a sum of labeled trivalent graphs with coefficients in $\mathbb{C}$ as illustrated in figure 30. Note that*
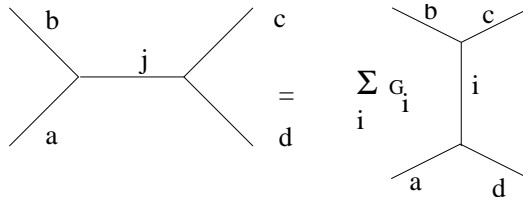

Figure 30: Graph exchange (exchanging a H-shaped graph for an I-shaped graph)

$$G_i = \frac{Tet \begin{bmatrix} a & b & i \\ c & d & j \end{bmatrix} \Delta_i}{\theta(a,d,i)\theta(b,c,j)} \qquad (12)$$

Proof: [9]. ∎

Remark 5.1. *One of the formulas given in section 3 is a special case of the recoupling theorem. In particular, if $j = 0$, we obtain the fusion formula from section 3.*

We now prove a theorem that demonstrates a sum of H-shaped trivalent graphs can be rewritten as a sum of I shaped trivalent subgraphs. This procedure gives the appearance of sliding edges past the vertices of the trivalent graph. Using the recoupling theorem, we may transform any trivalent graph without virtual crossings into a sum of weighted *string of beads* graphs as illustrated in figure 31.
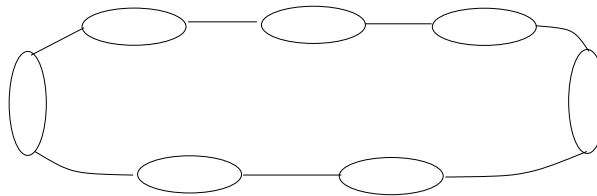

Figure 31: Example: String of Beads Graph

Lemma 5.2 (Trivalent Graphs). *A classical knot diagram may be transformed into a string of beads graph by replacing each classical crossing with a trivalent subgraph and applying the recoupling theorem.*

Remark 5.2. *This result follows from the fact that thickening an I-shaped and a H-shaped graph produces two homeomorphic surfaces. The surface produced by thickening any planar graph is a n-punctured sphere. The punctured sphere deformation retracts to a string of beads graph after homeomorphism. We will generalize this approach to show that virtual link diagrams correspond to a specific type of trivalent graphs. This lemma will be proved as a sub case of Lemma 5.3. Refer to [9], p. 115.*

The recoupling formula allows us to translate any planar trivalent graph (no virtual crossings) into a string of beads graph. This fact restricts the types of subgraphs that occur (in graphs obtained from classical link diagrams) to a small number of possibilities. As a result, we need only compute formulas that determine the WRT of the classical tangle diagrams that correspond these labeled subgraphs. In particular, it is sufficient to compute the coefficients that correspond to the insertion and deletion of θ-net subgraphs.

The reduction to a simple string of beads does not hold for virtual link diagrams. We can remove all classical crossing from the diagram by exchanging the classical crossings for H or I shaped trivalent subgraphs, and obtain a trivalent graph with only virtual crossings. However, we can not remove all virtual crossings by applying the recoupling theorem. For example, the graph shown in figure 32 can not be reduced to a trivalent graph without virtual crossings.
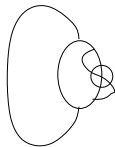

Figure 32: Unreduceable super bead

The reduced form of a virtual knot diagram is similar to a string of beads graph but includes three different types of beads. The reduced form of the virtual knot diagram is a string of *super beads*, *twisted beads* and *beads*. We illustrate the possible three bead types from the virtual case in figure 33.
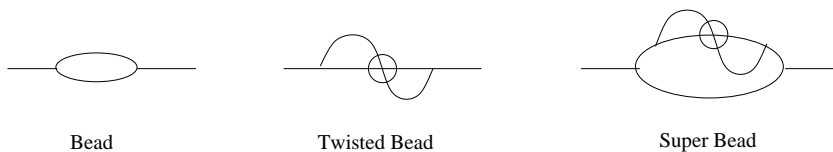

| Bead | Twisted Bead | Super Bead |

Figure 33: Beads types formed by virtual knot diagrams

We prove that the WRT of a virtual link diagram is equal to a weighted sum of the Jones polynomial of virtual link diagrams. The virtual link diagrams are indicated by labeled virtual string of beads graphs. These string of bead graphs are obtained from the virtual link diagram by applying the recoupling theorem

and crossing exchange. We first prove a lemma that demonstrates any trivalent graph with virtual crossings can be transformed into a string of the three bead types by sliding edges.

Lemma 5.3 (Graphical Lemma). *Any trivalent graph with virtual crossings may be reduced to a trivalent string of beads graph with three possible types of beads: the standard bead, twisted bead, and super bead. This graph will contain at most one twisted bead.*

Proof: Thicken the graph so that the graph is the core of a compact oriented surface, $T(G)$. An example of a graph and its corresponding thickened surface is shown in figure 34. Note that we may apply homeomorphisms these surfaces and the surfaces do not depend on the choice of embedding in 3 dimensional space. The two surfaces on the right hand side of figure 34 are equivalent.
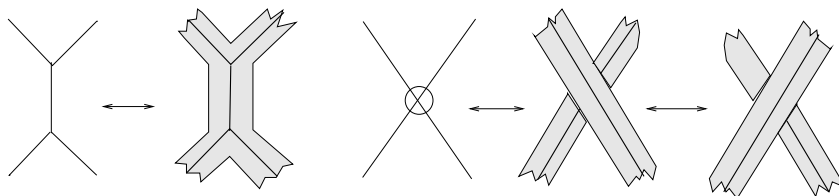

Figure 34: Thickened graph

Note that if the graph, G has $2n$ vertices, then G has $3n$ edges since the graph is trivalent. The Euler characteristic of the surface, $T(G)$ is $-n$ (since G is a deformation retract of T(G)). Without loss of generality, we assume that the surface has k boundary components.

Recall the following theorem from [5].

Theorem 5.4 (Surface Classification). *Let M be a connected, compact, orientable surface of Euler characteristic χ. Suppose ∂M has $k \geq 0$ boundary components. Then $\chi + k$ is even. Let $p = 1 - \frac{(\chi+k)}{2}$ then M is diffeomorphic to the surface obtained from an orientable surface of genus p by the removal of the interiors of k disjoint disks.*

Applying Theorem 5.4, $\chi(S) + k = -n + k$ and $-n + k$ is even. Let $p = 1 - \frac{-n+k}{2}$. We observe that $T(G)$ is the connected sum of p tori with k punctures. Each torus component contributes a handle pair. Each handle pair corresponds to a either a twisted bead or part of a super bead depending on the number of punctures. Each punctured disk forms a either plain bead or part of a super bead as shown in figures 35 and 36.

For example, a surface with one handle pair and one puncture corresponds to a single twisted bead on a loop (the graph shown in figure 32). The connected sum of three tori with one puncture and its corresponding graph are shown in figure 37.

After isotopy, any surface that is the connected sum of p tori with k punctures as may be regarded as a series of p handle pairs attached to a disk with $k - 1$
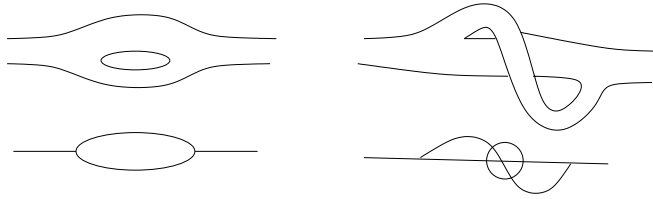
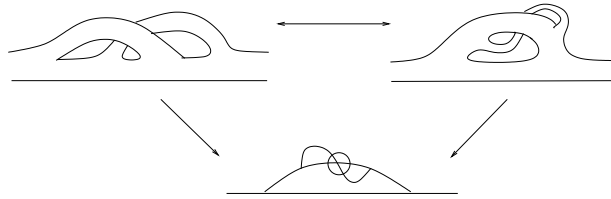Figure 35: Surfaces corresponding to the standard bead and the twisted bead

Figure 36: Surfaces corresponding to the super bead

punctures. As a result, these surfaces deformation retract to a string of beads type trivalent graph with standard beads, twisted beads, and a single super bead. ∎

Theorem 5.5 (Virtual Recoupling Theorem). *Let K be a labeled virtual link diagram. Using the recoupling theorem and crossing expansion, we may transform the virtual link diagram into a sum of labeled trivalent, string of beads graphs with coefficients in $\mathbb{C}$. The WRT of the labeled virtual link diagram is equal to the WRT of the sum of weighted trivalent graphs.*

Proof: From the previous theorem, it is clear that we can transform a virtual link diagram into a string of beads graph using the recoupling theorem and crossing expansion without coefficients. After determining this sequence of transformations, apply the appropriate coefficients and labels indicated by the
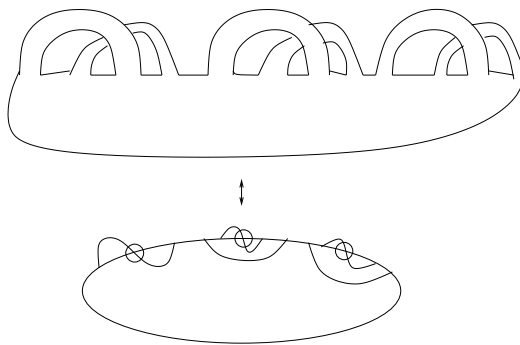

Figure 37: A surface and its corresponding graph

recoupling theorem, the crossing expansion formula, and the initial labeling of the link. ∎

5.1 Obstruction to Weight Formulas

Recall that the nth Jones-Wenzl idempotent has the property that $T_n U_i = 0$ for any elementary n-tangle U_i. We cannot easily extend the evaluation formulas given earlier in this paper because the Jones-Wenzl projector does not necessarily have the property that $T_n P_n = 0$ when P_n is a n-tangle with only virtual crossings. In the classical case, we relied on this fact to simplify the recursive formulas. The recursion formulas needed to determine the value of the Jones polynomial of $T_n P_n$ depend on the position of the virtual crossings. The evaluation of these formulas requires that we know the Jones polynomial of the closure of $T_{n-1} P_{n-1}$ for all $(n-1)$-tangles P_{n-1} containing only virtual crossings. We prove two theorems that indicate the complexity involved in computing the Jones polynomial of $T_n P_n$

Theorem 5.6. *The nth J-W projector, T_n, does not annihilate all n-tangles P_n with only virtual crossings.*

To prove Theorem 5.6 we need only demonstrate that $T(T_n E) \neq 0$ where E is a n-tangle with a single virtual crossing. We postpone this proof until after the proof of Lemma 5.9.

We introduce the following propositions preliminary to the proof of Theorem 5.6. The formulas in these propositions determine the number of the Jones polynomial of the closure $T_n P_n$.

Proposition 5.7. *If P is a (n-1)-tangle with only virtual crossings, we construct a n-tangle, P_n^*, by attaching an additional strand on the right. Then the Jones polynomial of the closure of $T_n P^*$ is determined by the following formula.*

$$T_n P = T_{n-1} P - \frac{\Delta_{n-2}}{\Delta_{n-1}} T_{n-1} P$$

Proof: Apply the recursion relation shown in figure 38. ∎

Proposition 5.8. *Let P be a n-tangle with only virtual crossings. We compute $T_n P$ recursively, and the depth of the recursion equation depends on the initial position of the rightmost strand in the n-tangle P.*

Proof: Let P be an n-tangle with only virtual crossings. We compute $T_n P$ recursively as shown in figures 38 and 39. We expand the diagram as in indicated in figure 39. The complexity of the recursion depends on the virtual crossings in P ∎

Remark 5.3. *The question of handling this recursion in a systematic way is an interesting research question.*
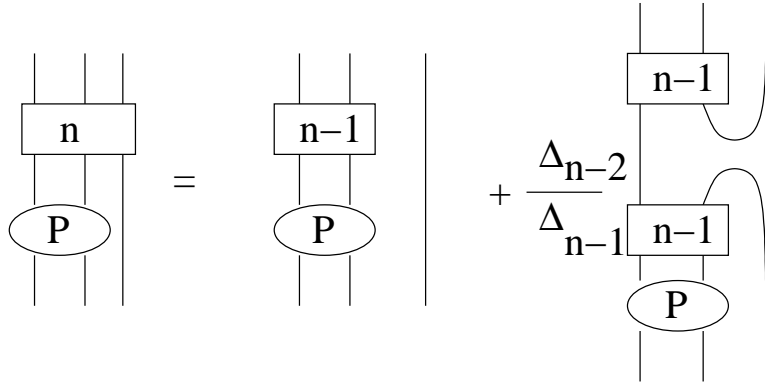
Figure 38: Diagrammatic proof of Proposition 5.7

Lemma 5.9. *Let E denote the n-tangle with a single virtual crossing involving only the 1st and the 2nd strands. Then:*

$$d\langle cl(T_n E)\rangle = (d + \frac{\Delta_{n-2}}{\Delta_{n-1}})\dots(d + \frac{\Delta_1}{\Delta_2})(d - 1)$$

Proof: We apply formula from Proposition 5.7 to $T_n E$. We calculate $\langle cl(T_2 E)\rangle = 1 - 1/d$. ∎

We now prove Theorem 5.6.

Proof of Theorem 5.6: If T_n is an idempotent, then $T_n E = 0$. However, $\langle cl(T_n E)\rangle \neq 0$ indicating that $T_n E$ is not the empty diagram. ∎

The algebra generated by extending n-tangle diagrams by including virtual crossings is a diagrammatic version of the Brauer algebra. Note that each classical n-tangle diagram is expanded (via the bracket) into an element of the Temperly-Lieb algebra. It is this extension of the Temperly-Lieb algebra by virtual elements that is isomorphic to the Brauer alegebra. The Brauer algebra is described in [1]. We would like to understand the structure of the Jones-Wenzl projectors in the context of the Brauer algebra. Results in this area would help in understanding the extension of the WRT invariant that we have discussed in this paper.
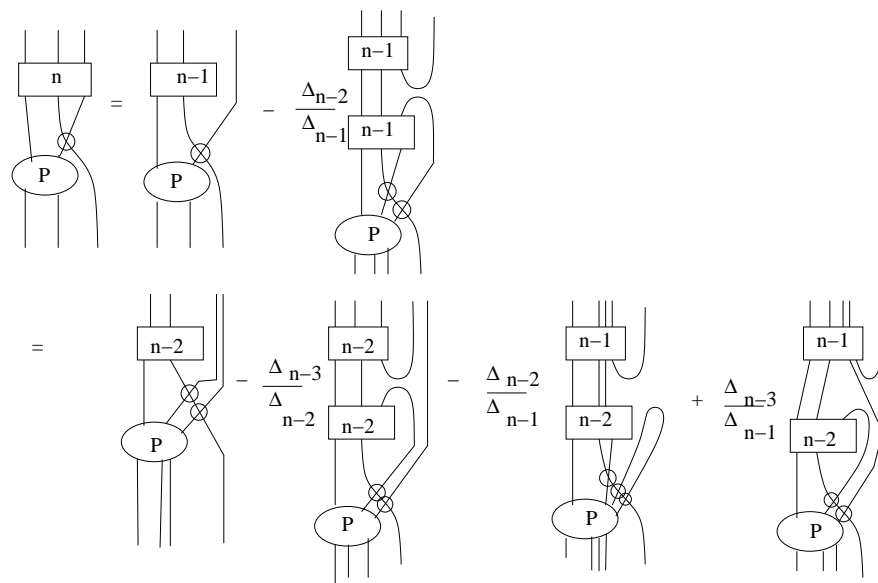
Figure 39: Diagrammatic proof of Proposition 5.8

References

[1] Georgia Benkart, Commuting actions—a tale of two groups, Contemporary Mathematics, American Mathematical Society, Vol. 194, p. 1-46, 1996, Lie algebras and their representations (Seoul, 1995)

[2] J. Scott Carter, Seiichi Kamada, and Masahico Saito, Stable equivalence of knots on surfaces and virtual knot cobordisms, Knots 2000 Korea, Vol. 1 (Yongpyong), J. Knot Theory Ramifications 11 (2002), no. 3, 311–32

[3] Heather A. Dye and Louis H. Kauffman, Minimal surface representations of virtual knots and links, www.arxiv.org, GT/0401035

[4] Mikhail Gussarov, Michael Polyak, and Oleg Viro Finite Type Invariants of Classical and Virtual Knots, Toplogy 39 (2000), no. 5 p. 1045-1068

[5] Morris W. Hirsch, Differential Topology, Springer-Verlag, Graduate Texts in Mathematics, 1997

[6] Naoko Kamada and Seiichi Kamada, Abstract link diagrams and virtual Knots, Journal of Knot Theory and it's Ramifications, Vol. 9 No. 1, p. 93-109, World Sci. Publishing, 2000

[7] Louis H. Kauffman, Detecting Virtual Knots, Atti del Seminario Matematico e Fisico dell'Universite di Modena, Vol. 49, suppl., p. 241-282, Univ. Modena, 2001

[8] Louis H. Kauffman, Virtual Knot Theory, European Journal of Combinatorics, Vol. 20, No. 7, p. 663-690, Academic Press, 1999

[9] Louis H. Kauffman and Sostenes L. Lins, Temperly-Lieb Recoupling Theory and Invariants of 3-Manifolds, Annals of Mathematics Studies, Princeton University Press, 1994

[10] Greg Kuperberg, What is a Virtual Link?, Algebr. Geom. Topol. 3 (2003), p. 587-591 (electronic) www.arxiv.org, GT/0208039

[11] Vassily O. Manturov, Kauffman-Like Polynomial and Curves in 2-Surfaces Journal of Knot Theory and its Ramifications, Vol. 12 (2003), no. 8, p. 1145-1153

[12] Viktor V. Prasolov and Alexei B. Sossinsky, Knots, Links, Braids and 3-Manifolds; An Introduction to New Invariants in Low-Dimensional Topology, American Mathematical Society, Translations of Mathematical Monographs, 1996

[13] Nikolai Yu Reshetikhin and Vladimir G. Turaev, Invariants of 3-manifolds via link polynomials and quantum groups, Inventiones Mathematicae, Vol. 103, No. 3, p. 547-597 , Springer, 1991

[14] Nikolai Yu Reshetikhin and Vladimir G. Turaev, Ribbon Graphs and their invariants derived from quantum groups, Communications in Mathematical Physics, Vol. 127, No. 1, p. 1-26, Springer, 1990,

[15] Edward Witten, Quantum field theory and the Jones polynomial, Braid group, knot theory and statistical mechanics, II, p. 361-451, Adv. Ser. Math. Phys., 17, World Sci. Publishing 1994